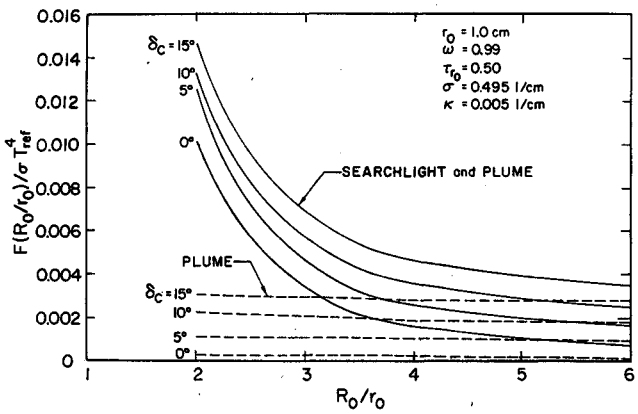

Fig. 4 Heating of rocket base due to a conical, isothermal, isotropic scattering, $\omega = 0.99$ plume. Effect of searchlight emission and plume cone angle for $\tau_{r_0} = 0.5$ and $z_0 = 0$.

In other words, the temperature of the plume in the nozzle is the same as the temperature of the exhaust plume. If the temperature in the nozzle were twice the plume temperature, the searchlight emission would increase by a factor of 16. The figures show searchlight emission can be very important. The percentage of heating due to searchlight emission decreases as both δ_c and R_0/r_0 increase.

As the plume albedo increases toward one, the plume emission decreases and the searchlight emission increases. In the limit of $\omega = 1$, the radiation at R_0/r_0 will be entirely due to searchlight effects (see Fig. 2). The general trends are that as δ_c increases, radiative heating increases and as ω increases radiative heating decreases. Searchlight radiation can become important for highly scattering, low emitting plumes at small R_0/r_0.

The computer run time varies with the number of photons that are input per grid point on the plume surface and with the number of grid points. A typical run time to calculate the radiation at one R_0/r_0 position is 20 s on an IBM 4381 computer, for 200 photons/(grid point) and 200 grid points (40,000 photons) for the results presented herein.

Conclusions

Backward Monte Carlo calculations work well for radiation base heating predictions and the predictions agree well with previously published results for similar problems. For isothermal, gray plumes the radiative base heating increases as plume cone angles increase. As the plume albedo increases from zero toward one, the radiative heating decreases. Searchlight radiative heating becomes important as the plume albedo increases. It is generally more important at small values of R_0/r_0 and decreases as R_0/r_0 increases. In more realistic, variable property plumes, the albedo is a local value, but the same trends will occur. As the scattering becomes more significant the average albedo increases and searchlight radiation will become more important.

Acknowledgments

This work was partially supported by Remtech Inc., Huntsville, Alabama. The backward Monte Carlo code was obtained from Robert A. Reed, Sverdrup Technology, Inc., Arnold Air Force Base, TN.

References

[1]Rochelle, W. C., "Review of Thermal Radiation from Liquid and Solid Propellant Rocket Exhausts," NASA TMX 53579, Feb. 1967.

[2]Carlson, D. J., "Radiation from Rocket Exhaust Plumes, Part II: Metalized Solid Propellants," AIAA 2nd Propulsion Joint Specialist Conference, Colorado Springs, CO, AIAA Paper 66-652, June 13–17, 1966.

[3]Fontenot, J. E., Jr., "Thermal Radiation from Solid Rocket Plumes at High Altitude," *AIAA Journal*, Vol. 3, No. 5, 1965, pp. 970–972.

[4]Morizumi, S. J., and Carpenter, H. J., "Thermal Radiation from the Exhaust Plume of an Aluminized Composite Propellant Rocket," *Journal of Spacecraft and Rockets*, Vol. 1, No. 5, 1964, pp. 501–507.

[5]Bartky, C. D., and Bauer, E., "Predicting the Emittance of a Homogeneous Plume Containing Alumina Particles," *Journal of Spacecraft and Rockets*, Vol. 3, No. 10, 1966, pp. 1523–1527.

[6]Bobco, R. P., and Edwards, R. H., "Radiation from an Absorbing Scattering Conical Dispersion with Non-Uniform Density," Aerospace Technology Research Report, SSD 60571R, Hughes Aircraft Co., Los Angeles, CA, 1966.

[7]Gorshkova, S. N., "Radiative Heat Transfer in a Truncated Cone Chamber in which the Heat Source Lies within the Gas Space," *Heat Transfer—Soviet Research*, Vol. 18, No. 1, 1986, pp. 39–43.

[8]Kaminski, D. A., "Radiative Heat Transfer from a Gray, Absorbing-Emitting Medium in a Conical Enclosure," *Proceedings of the 1988 American Society of Mechanical Engineers National Heat Transfer Conference*, HTD-Vol. 96, 1988, pp. 201–207.

[9]Lin, J. D., and Wang, C. S., "Radiative Heat Transfer from an Absorbing and Isotropically Scattering Medium Contained within a Truncated Cone," *American Society of Mechanical Engineers National Heat Transfer Conference*, HTD-Vol. 106, Heat Transfer Phenomena in Radiation, Combustion and Fires, edited by R. K. Shah, 1989, pp. 205–211.

[10]Bobco, R. P., "Radiation from Conical Surfaces with Nonuniform Radiosity," *AIAA Journal*, Vol. 4, No. 3, 1966, pp. 544–546.

[11]Bobco, R. P., "Reply by Author to D. K. Edwards on Radiation from Conical Surfaces with Nonuniform Radiosity," *AIAA Journal*, Vol. 7, No. 8, 1969, p. 1659.

[12]Edwards, D. K. "Comment on Radiation from Conical Surfaces with Nonuniform Radiosity," *AIAA Journal*, Vol. 7, No. 8, 1969, pp. 1656–1658.

[13]Edwards, D. K., and Bobco, R. P., "Effect of Particle Size Distribution on the Radiosity of Solid Propellant Rocket Motor Plumes," Spacecraft Radiative Transfer and Temperature Control, edited by T. E. Horton, Vol. 83, Progress in Astronautics and Aeronautics, AIAA, New York, 1982, pp. 169–188.

[14]Edwards, D. K., Sakurai, Y., and Babikan, D. S., "A Two-Particle Model for Rocket Plume Radiation," *Journal of Thermophysics and Heat Transfer*, Vol. 1, No. 1, 1987, pp. 13–20.

[15]Watson, G. H., and Lee, A. L., "Thermal Radiation Model for Solid Rocket Booster Plumes," *Journal of Spacecraft and Rockets*, Vol. 14, No. 11, 1977, pp. 641–647.

[16]Tien, C. L., and Abu-Romia, M. M., "A Method of Calculating Rocket Plume Radiation to the Base Region," *Journal of Spacecraft and Rockets*, Vol. 1, No. 4, July–Aug., 1964, pp. 433–435.

[17]Nelson, H. F., "Modeling for Rocket Plume Base Heating Calculations," 19th JANNAF Plume Technology Conference, U.S. Army Missile Command, Redstone Arsenal, AL, May 14–16, 1991. Chemical Propulsion Information Agency, CPIA Publication 568, May 1991, pp. 585–592.

[18]Stockham, L. W., and Love, T. J., "Radiative Heat Transfer from a Cylindrical Cloud of Particles," *AIAA Journal*, Vol. 6, No. 10, 1968, pp. 1935–1940.

Free Convection About Vertical Needles Embedded in a Saturated Porous Medium

Chunmei Peng,* Taofang Zeng†, and Gang Chen‡
Huazhong University of Science and Technology, Wuhan, People's Republic of China

Nomenclature

a = size of needle
C = constant

Received April 1, 1991; revision received Sept. 4, 1991; accepted for publication Sept. 5, 1991.

*Assistant Professor, Department of Power Engineering; currently, Engineer of Wuhan Boiler Works.

†Graduate Student; Department of Engineering Mechanics, Tsinghua University, Beijing.

‡Teaching Assistant; currently, Ph.D. Candidate, Department of Mechanical Engineering, University of California, Berkeley.

c_p = specific heat of fluid
f = reduced stream function
g = gravitational acceleration
K = permeability of porous medium
k_m = thermal conductivity of porous medium
n = power index
p = pressure
q = surface heat flux
$R(x)$ = surface shape of needle
R_{ax} = modified local Rayleigh number
T = temperature
u, v = velocity components
α = equivalent thermal diffusivity ($\alpha = k_m/(\rho C_p)_f$)
β = coefficient of thermal expansion
ψ = stream function
η = similarity variable
μ = fluid's dynamic viscosity
ν = fluid's kinematic viscosity
ρ = density of fluid
θ = dimensionless temperature

Subscripts
f = fluid
w = on the surface
∞ = at infinity

Introduction

THE study of free convection about the outer surface of a vertical needle embedded in a saturated porous medium has important engineering applications. Minkowycz and Cheng[1] have studied the free convection about a vertical cylinder embedded in a porous medium, where the surface temperature of the cylinder varies as a power function of distance from the leading edge. Cheng[2] also considered mixed convection from a horizontal surface embedded in a porous medium and obtained a similarity solution. Laminar natural convection of a Newtonian fluid from slender needles with axial power-law wall heat flux variation was studied by Chen.[3] Merkin,[4] Cheng,[5] and Huang and Chen[6] investigated the effect of surface mass transfer on free convection in a porous medium. Vafai and Tien,[7] and Nagendra et al.[8] have analyzed boundary and inertia effects on flow and heat transfer in porous media. Recently, Nakayama et al.[9] dealt with non-Darcy free convection flows using the Ergun model. Lee et al.[10] and Heckel et al.[11] employed a weighted finite-difference method to solve the transformed system of equations and presented the results of free convection along slender vertical cylinders immersed in a Newtonian fluid with variable surface temperatures and variable surface heat flux. Recently, Lai et al.[12] presented results for free and mixed convection about needles in a porous medium with surface temperatures that vary as a power function of the distance from the leading edge.

The objective of this paper is to present an analysis of free convection from slender needles embedded in a saturated porous medium where axial wall heat flux of the needle varies as a power-law function of distance from the leading edge. Similarity velocity and temperature profiles as well as heat transfer results are obtained by introducing a new transformation parameter for three different needles.

Mathematic Formulation

Consider the problem of steady free convection about a vertical needle embedded in a saturated porous medium with the assumptions that the convection fluid and the porous medium are isotropic, in thermal equilibrium, and have constant physical properties and that the Boussinesq approximation is employed. The governing equations from Minkowycz and Cheng[1] are

$$\frac{\partial(ru)}{\partial x} + \frac{\partial(rv)}{\partial r} = 0 \tag{1}$$

$$u = -\frac{K}{\mu}\left(\frac{\partial p}{\partial x} + \rho g\right) \tag{2}$$

$$v = -\frac{K}{\mu}\frac{\partial p}{\partial r} \tag{3}$$

$$u\frac{\partial T}{\partial x} + v\frac{\partial T}{\partial r} = \alpha\cdot\left[\frac{1}{r}\frac{\partial}{\partial r}\left(r\frac{\partial T}{\partial r}\right) + \frac{\partial^2 T}{\partial x^2}\right] \tag{4}$$

$$\rho = \rho_\infty[1 - \beta(T - T_\infty)] \tag{5}$$

The appropriate boundary conditions are

at surface

$$r = R(x), \qquad v = 0, \qquad q = -k_m\frac{\partial T}{\partial r} = Cx^n \tag{6}$$

at infinity

$$r \to \infty, \qquad u = 0, \qquad T = T_\infty \tag{7}$$

where $C > 0$. In Eq. (6), the prescribed wall heat flux is assumed to be a power function of distance from the leading edge.

The continuity equation is automatically satisfied by the stream function ψ as

$$ru = \frac{\partial\psi}{\partial r}, \qquad rv = -\frac{\partial\psi}{\partial x} \tag{8}$$

The governing equations and boundary conditions in terms of ψ and T are given by

$$\frac{\partial}{\partial r}\left(r\frac{\partial\psi}{\partial r}\right) + \frac{1}{r}\frac{\partial^2\psi}{\partial x^2} = \frac{\rho_\infty\beta Kg}{\mu}\frac{\partial T}{\partial r} \tag{9}$$

$$\frac{\partial\psi}{\partial r}\frac{\partial T}{\partial x} - \frac{\partial\psi}{\partial x}\frac{\partial T}{\partial r} = \alpha\left[\frac{\partial}{\partial r}\left(r\frac{\partial T}{\partial r}\right) + r\frac{\partial^2 T}{\partial x^2}\right] \tag{10}$$

$$r = R(x): \frac{\partial\psi}{\partial x} = 0, \qquad q_w = Cx^n \tag{11}$$

$$r \to \infty: \frac{\partial\psi}{\partial r} = 0, \qquad T = T_\infty \tag{12}$$

If the boundary-layer approximation is applied, Eqs. (9) and (10) become

$$\frac{\partial}{\partial r}\left(r\frac{\partial\Psi}{\partial r}\right) = \frac{\rho_\infty\beta gK}{\mu}\frac{\partial T}{\partial r} \tag{13}$$

$$\frac{\partial\psi}{\partial r}\frac{\partial T}{\partial x} - \frac{\partial\psi}{\partial x}\frac{\partial T}{\partial r} = \alpha\frac{\partial}{\partial r}\left(r\frac{\partial T}{\partial r}\right) \tag{14}$$

The following dimensionless variable is introduced:

$$\eta = R_{ax}^{2/3}\cdot r^2/x^2 \tag{15}$$

where $R_{ax} = Kg\beta qx^2/(k_m\alpha\nu)$ is the modified local Rayleigh number.

On the surface, $\eta = a$, Eq. (15) becomes

$$r = R(x) = \left(\frac{k_m\alpha\nu}{Kg\beta C}\right)^{1/3}\cdot x^{\frac{1-n}{3}}\cdot a^{1/2} \tag{16}$$

From Eq. (16) we know that the size of the needle is determined by parameter a; the shape of the body or the relationship between $R(x)$ and x is dependent on n.

Table 1 Values of $\theta^{-1}(a)$

a	0.02			0.10			0.50		
n	−1.0	0.0	1.0	−1.0	0.0	1.0	−1.0	0.0	1.0
$\theta^{-1}(a)$	2.4390	3.0121	3.4294	1.3158	1.5625	1.7243	1.0799	1.2346	1.3333

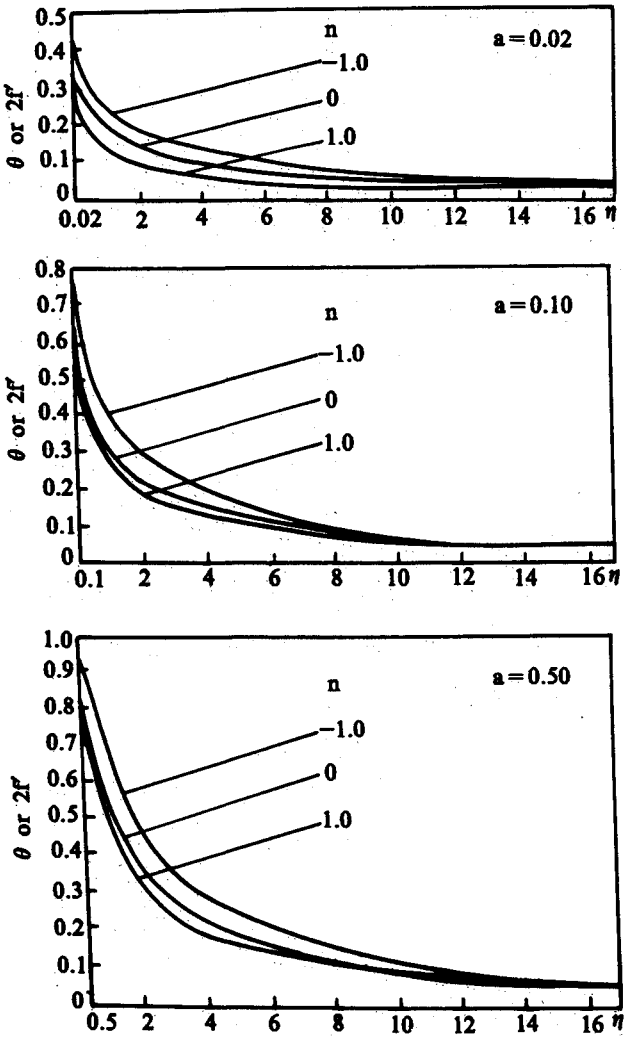

Fig. 1 Dimensionless temperature distribution.

We now introduce the similarity variables:

$$\psi(x, r) = \alpha x f(\eta) \tag{17}$$

$$\theta(\eta) = R_{ax}^{1/3} \cdot \frac{T - T_\infty}{xq/k_m} \tag{18}$$

It can be shown that velocity components in terms of the new variables are

$$u = 2\alpha \frac{1}{x} R_{ax}^{2/3} \cdot f'(\eta) \tag{19}$$

$$v = -\frac{\alpha}{r}\left(f + \frac{2n-2}{3}\eta f'\right) \tag{20}$$

and the governing Eqs. (13 and 14) with the boundary conditions (11 and 12) in terms of new variables become

$$f'' = \tfrac{1}{2}\theta' \tag{21}$$

$$2\eta\theta'' + 2\theta' + f\theta' - \frac{2n+1}{3} f'\theta = 0 \tag{22}$$

$$\eta = a: f(a) = -\frac{2n-2}{3} a f'(a)$$

$$\theta'(a) = -\frac{1}{2a^{1/2}} \tag{23}$$

$$\eta \to \infty: f'(\infty) = 0, \qquad \theta(\infty) = 0 \tag{24}$$

Results and Discussion

Integrating Eq. (21) from η to infinity, we get

$$f' = \tfrac{1}{2}\theta \tag{25}$$

Using Eq. (25), Eq. (22) yields

$$2\eta f''' + (2 + f)f'' - \frac{2n+1}{3} f'^2 = 0 \tag{26}$$

The appropriate boundary conditions at $\eta = a$ are

$$f''(a) = \frac{1}{2}\theta'(a) = -\frac{1}{4a^{1/2}} \tag{27a}$$

$$f(a) = -\frac{2n-2}{3} a f'(a) \tag{27b}$$

Equations (26), (27), and (24) can be integrated numerically by means of the Runge-Kutta method incorporated with the shooting techniques for a systematic guessing of $\theta(a)$.

Figure 1 shows that the values of θ or $2f'$ decrease from 1 to 0 as η is increased from zero at different values of a.

The local Nusselt number is defined as

$$Nu_x = \frac{hx}{K_m} = \frac{q_w x}{K_m(T_w - T_\infty)} = R_{ax}^{1/3}\theta^{-1}(a)$$

where the value of $\theta^{-1}(a)$ is tabulated in Table 1.

In Table 1, the parameter n denotes: 1) $n = 1.0$: a cylinder with linear wall heat flux distribution; 2) $n = 0.0$: a blunt-nosed needle with uniform wall heat flux; and 3) $n = -1.0$: a sharp-nosed needle with wall heat flux varying as x^{-1}.

It can be seen from this table that, in addition to R_{ax}, the needle size and shape combined with wall heat flux variation have significant effects on the surface heat transfer. For a given shape, the smaller the size, the larger the Nu_x. Among the three cases considered, the cylinder with a linear wall heat flux yields the highest surface heat transfer rate.

Conclusions

1) Free convection from vertical needles embedded in a saturated porous medium with power-law surface heat flux can be solved by the similarity method.

2) Needle size and shape have strong effects on both flow and heat transfer. Thinner needles produce higher surface heat transfer rate.

3) In the scope of computation, the heat transfer has higher rate as n increases.

4) The local Nusselt number is proportional to the third root of Rayleigh number.

References

[1]Minkowycz, W. J., and Cheng, P., "Free Convection About a Vertical Cylinder Embedded in a Porous Medium," *International*

Journal of Heat and Mass Transfer, Vol. 19, No. 7, 1976, pp. 805–813.

[2]Cheng, P., "Similarity Solution for Mixed Convection from Horizontal Impermeable Surface in Saturated Porous Media," *International Journal of Heat and Mass Transfer*, Vol. 20, No. 9, 1977, pp. 893–898.

[3]Chen, J. L. S., "Natural Convection from Needles with Variable Heat Flux," *Journal of Heat Transfer*, Vol. 105, No. 2, 1983, pp. 403–406.

[4]Merkin, J. H., "Free Convection Boundary Layers in a Saturated Porous Medium with Lateral Mass Flux," *International Journal of Heat and Mass Transfer*, Vol. 21, No. 9, 1978, pp. 1499–1504.

[5]Cheng, P., "The Influence of Lateral Mass Flux on Free Convection Boundary Layers in a Saturated Porous Medium," *International Journal of Heat and Mass Transfer*, Vol. 20, No. 3, 1977, pp. 201–206.

[6]Huang, M. J., and Chen, C. K., "Effect of Surface Mass Transfer on Free Convection Flow over Vertical Cylinder Embedded in a Saturated Porous Medium," *Journal of Energy Resources Technology*, Vol. 107, No. 3, 1985, pp. 394–396.

[7]Vafai, K., and Tien, C. L., "Boundary and Inertia Effects on Flow and Heat Transfer in Porous Media," *International Journal of Heat and Mass Transfer*, Vol. 24, No. 2, 1981, pp. 195–203.

[8]Nagendra, H. R., Tirunarayanan, M. A., and Ramachandran, A., "Laminar Free Convection from Vertical Cylinders with Uniform Heat Flux," *Journal of Heat Transfer*, Vol. 92, No. 1, 1970., pp. 191–194.

[9]Nakayama, A., Koyama, H., and Kuwahara, F., "Similarity Solution for non-Darcy Free Convection from a Nonisothermal Curved Surface in a Fluid-Saturated Porous Medium," *Journal of Heat Transfer*, Vol. 111, No. 3, 1989, pp. 807–811.

[10]Lee, H. R., Chen, T. S., and Armaly, B. F., "Natural Convection along Slender Vertical Cylinders with Variable Surface Temperature," *Journal of Heat Transfer*, Vol. 110, No. 1, 1988, pp. 103–108.

[11]Heckel, J. J., Chen, T. S., and Armaly, B. F., "Natural Convection along Slender Vertical Cylinders with Variable Surface Heat Flux," *Journal of Heat Transfer*, Vol. 111, No. 4, 1989.

[12]Lai, F. C., Pop, I., and Kularki, F. A., "Free and Mixed Convection from Slender Bodies of Revolution in Porous Media," *International Journal of Heat and Mass Transfer*, Vol. 33, No. 8, 1990, pp. 1767–1769.

Rotational Temperature Measurements in an Arc Jet

G. Cernogora,* G. Gousset,† and L. Hochard*
Université Paris-Sud, 91405 Orsay, France
and
M. Dudeck,‡ P. Lasgorceix,§ and V. Lago¶
Centre National de la Recherche Scientifique, 92190 Meudon, France

Introduction

IN order to simulate the flow conditions around a space vehicle during its hypersonic atmospheric re-entry, a low pressure arc jet is used to create high temperature and high speed flow.[1] It is important to know the physical and chemical conditions of the flow in this jet. The temperatures are important physical parameters to evaluate the degree of simulation of this ground device and to calculate specific chemical rates and transport coefficients. The temperatures are about a few thousands of degrees. We need to design accurate and nonintrusive diagnostics for high temperature measurements in these flow conditions.

In the low pressure arc jet, the plasma is not expected to be in thermal equilibrium. To obtain the jet temperature, gas flow can be excited with a high energy electron beam in order to observe the re-emitted light. This technique can be used for nonionized gas flow.[2] Because plasma jets are luminous, it is not necessary to excite the flow. In these conditions it is possible to determine plasma vibrational distributions and rotational temperatures from optical emission spectroscopy (OES).[3] Using high resolution spectroscopy, Bacri and Lagreca[4] have measured rotational temperatures in an atmospheric nitrogen arc. Using the same technique Blackwell et al.[5] have evaluated temperature in a shock layer. They have used a low resolution monochromator and have recorded mainly vibrational spectra without rotational resolution. This paper presents a new attempt for optical emission spectroscopy measurement of temperature from high resolution spectra in a low pressure arc.

Experiment

The nitrogen arc jet is produced in the Aerothermique Laboratory SR1 wind tunnel (Fig. 1). The plasma is produced, with a vortex stabilized dc arc, between a thoriated 2% tungsten cathode and a copper anode used as a nozzle. Typical flow conditions are: arc discharge current from 50–150 A; gas flow rate from 5–15 liters/min (0.1–0.3 g/s); static pressure from 0.1–10 Torr; velocity from 2000–5000 m/s. In order to investigate axial and longitudinal profiles, the plasma generator can be moved on a Cartesian axis. The plasma jet is stationary (several tens of hours) and large (length $\approx$ 1 m and diameter $\approx$ 0.5 m at a pressure of 13.3 Pa). The light emitted from the plasma, observed through a fused silica window, is focused by the fused silica lens on the entrance slit of a 150-cm focal length monochromator (Sopra). A 1200 lines/mm grating was used in this monochromator. In order to increase the signal over noise ratio, an optical chopper (300 Hz) modulated the light beam. The photomultiplier (Hamamatsu R928) output signal was detected by a lock-in amplifier (NF Electronics Instruments 5610B), tuned on the chopper modulation frequency, and connected to a microcomputer.

In this paper measurements are presented on the first negative system of nitrogen: $N_2^+(B^2\Sigma_u, v' = 0) \rightarrow N_2^+(X^2\Sigma_g, v'' = 0)$. This band, observed in the plasma jet, is also emitted

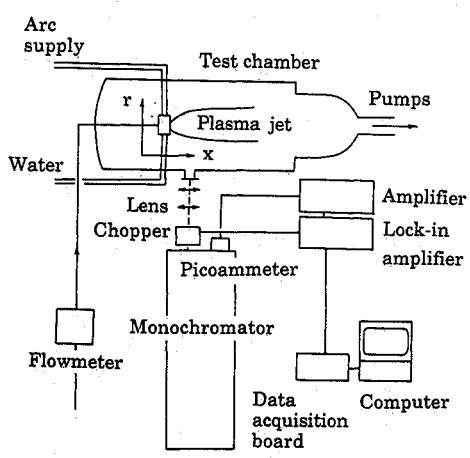

Fig. 1 Schematic of apparatus used for rotational temperature measurements.

Received Aug. 2, 1991; revision received Sept. 10, 1991; accepted for publication Sept. 10, 1991.

*Maître de Conférences, Laboratoire de Physique des Gaz et des Plasmas.

†Chargé de Recherches au Centre National de la Recherche Scientifique, Laboratoire de Physique des Gaz et des Plasmas.

‡Professor, Université de Paris 6, Laboratoire d'Aérothermique. Member AIAA.

§Chargé de Recherches au Centre National de la Recherche Scientifique, Laboratoire d'Aérothermique.

¶Graduate Student, Centre National de la Recherche Scientifique, Laboratoire d'Aérothermique.